

**Development of a Plasmid Containing the *Bacillus anthracis*  
*cotE* Gene**

Melissa Widel

**SENIOR HONORS THESIS**

Submitted In Partial Fulfillment of Requirements of the  
*College Scholars Honors Program*  
*North Central College*

May 15, 2017

Approved: \_\_\_\_\_ Date: \_\_\_\_\_  
*Thesis Director Signature*

Dr. Nancy Peterson

Approved: \_\_\_\_\_ Date: \_\_\_\_\_  
*Second Reader Signature*

Dr. Jonathan Visick

## **ABSTRACT**

Complex structures are formed and regulated by a network of gene and protein interactions. One such structure, the bacterial spore coat, is formed by sporulating members of the phyla Firmicutes, including species in the genus *Bacillus*. Formed in response to a harsh environment, a bacterial endospore is highly resistant due to this spore coat. The spore coat of *Bacillus* species can be used as a model system to study the role of genes in the formation and regulation of complex structures. In this study, development of a tool to study the morphogenic role of the *Bacillus* spore coat protein CotE began. Specifically, I worked to create a plasmid that would allow me to delete the *cotE* gene by homologous recombination resulting in an insertion event, thus allowing for the study of the role of CotE. A fragment of the *cotE* gene from *Bacillus anthracis* genomic DNA was amplified and ligated into an expression plasmid, which would allow for homologous recombination. Gel electrophoresis results indicate that the correct insert has been isolated, but successful insertion into the expression plasmid has yet to be confirmed. Once the correct plasmid is confirmed, transformation and homologous recombination can result in an insertion deletion of *cotE* in *B. anthracis*. The relative conservation of *cotE* across species of the genus *Bacillus* should allow for the same engineered plasmid to be used to knock out *cotE* in multiple species of *Bacillus*. Successful completion of this research would present this method as a viable manner of researching complex structures.

## **INTRODUCTION**

Complex structures, which are found throughout biological systems, are constructed and regulated by an intricate pattern of gene expression and protein interactions (Kim et al. 2006). Due to the intricate nature of these interactions, studying the role of a single gene and its

associated protein can prove difficult in complex structures. However, the near ubiquity of complex structures in biological systems makes such studies important, and the development of a method for studying a single gene involved in a complex structure could have a significant impact on research done in multiple subdisciplines. The bacterial spore coat, a multilayered protein and carbohydrate complex (Driks 2002), has been proposed as a model system for studying complex structures (Driks 1999; Driks 2004). As such, this research focuses on the development of a plasmid for use in studying the role of a single spore coat gene and its associated protein in species *Bacilli*, some of which are represented in a phylogenetic tree (Figure 1). After demonstrating the methodology's viability in the model system of the bacterial spore coat, it can be proposed as a method to study other complex structures.

**Overview of Bacterial Endospores.** Certain bacteria can form endospores in response to harsh environmental conditions, such as a lack of nutrients (Driks 2002). These endospores have no active metabolism, allowing them to survive in nutrient-poor conditions. Additionally, the multilayered bacterial spore coat makes endospores resistant to a variety of environmental factors (Nicholson et al. 2000), which will be further outlined in subsequent sections. In order to form an endospore, the following very general process occurs in the same manner in all endospore-forming bacteria: first, a septum forms in the original (mother) cell (Figure 2), dividing the cell into the mother cell and a smaller forespore (eventually becoming the endospore), which sit side by side (Driks 1999). Proteins and other molecules necessary for endospore formation are synthesized by both the mother cell and the forespore. The septum around the forespore then contracts and pinches off to form a circular compartment that sits within the mother cell (Driks 1999). The forespore encloses the core, which contains the bacterium's chromosome (Driks 2004). The forespore has two membranes surrounding it, and

those membranes serve as a framework upon which the spore coat will be constructed (Driks 1999). First, peptidoglycan, a carbohydrate and protein macromolecule which is the main component of the bacterial cell wall (Schleifer and Kandler 1972), is deposited between the two membranes, forming the cortex (Driks 2002). The inner coat is then built upon the cortex, followed by the outer coat (Driks 1999; Figure 3A-B). Both coat layers are mostly composed of proteins (Henriques and Moran 2007). Some endospore-formers, such as *Bacillus thuringiensis* and *B. subtilis* also have another layer surrounding the outer coat, called the exosporium (Driks 2004; Figure 3C-D). The exosporium is not deposited directly on top of outer coat. Instead, the two are separated by an interspace which forms a gap between the layers (Giorno et al. 2007). At this point, the endospore is fully formed, made up of (from inside to outside): the core, the inner membrane, the cortex, the outer membrane, the inner coat, the outer coat, and (in some species) the interspace and exosporium. The endospore is released via lysis of the mother cell (Driks 1999), where it can remain dormant until environmental conditions are more favorable.

**Role of Endospores.** As the mother cell and forespore must synthesize the proteins and other molecules necessary to deposit multiple layers to form an endospore, the process is resource- and energy-consuming. However, this process results in an endospore which is more likely to survive in harsh environmental conditions, and therefore more likely to pass on its genetic information, than the mother cell is. Once formed, bacterial endospores lack an active metabolism (Atrih and Foster 2002), and thus require no nutrients to survive. Endospores have also been shown to be highly resistant to desiccation (Nicholson et al. 2000), and therefore can survive in environments with minimal water available. Additionally, endospores can survive other environmental extremes not associated with a nutrient shortage. Endospores are known to be resistant to dry heat, wet heat, UV radiation, a variety of chemicals, and high pressure (Nicholson et al. 2000).

However, the spore coat itself is not the only characteristic responsible for an endospore's resistance. Additionally, endospores are dehydrated, leading to a low core water content. The mineral content of the endospore, specifically the divalent cation content, has also been shown to be involved in endospore resistance. The presence of  $\alpha/\beta$ -Type small acid-soluble spore proteins (SASP) have been shown to be involved in the protection of DNA. While these are all known to accompany the spore coat in contributing to the resistance of endospores, the extent and exact mechanisms responsible are not completely known (Nicholson et al. 2000).

Despite the protection provided by the multilayered spore coat, the spore coat must also allow the endospore to constantly sense the environmental conditions. An endospore monitors the environment for the presence of certain compounds indicative of favorable growth conditions, such as L-alanine, inorganic ions, or sugars, (Moir and Smith 1990). In the presence of such compounds, the spore can germinate, or return to vegetative growth. Thus, the spore must be flexible enough to allow for the spore to germinate (Driks 2004).

The balance between protection and flexibility is enabled by the complex structure of the spore coat and the genes and proteins involved in its formations.

**Spore-Forming Bacteria.** The phylum Firmicutes is the only phylum containing endospore-forming bacteria, though not all bacteria in Firmicutes are endospore-formers. Firmicutes contains five classes of bacteria: *Bacilli*, *Clostridia*, *Erysipelotrichia*, *Negativicutes*, and *Thermolithobacteria*. All except *Thermolithobacteria* include endospore-forming bacteria (Galperin 2013). As the classes are further subdivided into orders, families, genera, and species, endospore-forming bacteria are a diverse group. More commonly known endospore-forming bacteria include *Bacillus anthracis*, the causative agent of anthrax; *Bacillus subtilis*, which is

commonly used in research; *Clostridium botulinum*, the causative agent of botulism; and *Clostridium difficile*, which can cause diarrhea and colitis (Galperin 2013).

**Genes and Proteins Involved in Spore Coat Formation.** The genes involved in spore coat formation vary across the phylum Firmicutes. Many genes are not conserved across different classes (Onyenwoke et al. 2004) or even within the same genus (Alcaraz et al. 2010) of bacteria. Some genes involved in spore coat formation are conserved across multiple species in Firmicutes (Onyenwoke et al. 2004; Henriques and Moran 2007), but many more are present in only a subset of species. Despite the diversity of *Bacilli* species, the general formation of the spore coat is conserved and some proteins play major morphogenic roles in multiple species (Giorno et al. 2007; Henriques and Moran 2007; Liu et al. 2004; Bressuire-Isoard et al. 2016). For the purpose of this research, genes and proteins involved in *Bacillus* endospore formation will be focused on.

*B. subtilis* Sporulation. As *B. subtilis* is perhaps the most well-studied endospore-former, the genes involved in its spore coat formation have been established. Before formation of the septum, the sigma factors (RNA subunits which control transcription; Paget 2015)  $\sigma^{11}$  and  $\sigma^A$  are active and control gene expression in both the mother cell and what will become the forespore (Driks 1999). The transcription factor Spo0A (Spo indicates involvement in sporulation, while the genes are grouped using numbers and letters; Sandman et al. 1987) is also involved, mediating the expression of the genes encoding the proteins FtsZ and SpoIIE. FtsZ forms a ring that moves to one end of the mother cell, which will eventually form the septum. SpoIIE localizes to the forespore pole, while the protein SpoIIIE mediates the movement of the DNA into the forespore (Dworkin 2014). The  $\sigma^{11}$ -controlled protein SpoIIB (Driks 1999) localizes to the FtsZ ring during separation. SpoIIE may also be involved in the formation of the septum (Dworkin 2014). Following SpoIIB localization, SpoIIM, the autolysin SpoIIP, and the

peptidoglycan hydrolase SpoIID localize in the same area, forming the DMP complex. The DMP complex hydrolyzes the peptidoglycan between the forespore and the mother cell, allowing for proteins in the two compartments to interact (Dworkin 2014).

After the forespore and mother cell are successfully separated, mother cell-specific and forespore-specific proteins begin to be expressed. The different patterns of gene expression, controlled by sigma factors, in the endospore and the mother cell lead to the morphogenic differences between the two. SpoIIE is involved in the activation of the sigma factor  $\sigma^F$  in the forespore (Dworkin 2014), while the anti-sigma factor SpoIIAB ensures that  $\sigma^F$  remains inactive in the mother cell. The sigma factor  $\sigma^E$  then becomes active in the mother cell as pro- $\sigma^E$  is cleaved into its active form.  $\sigma^E$  leads to expression of the transcription factor SpoIIID (Driks 1999), SpoIVA, SpoVID (Dworkin 2014), the sigma factor  $\sigma^K$ , and the spore coat proteins CotE and CotJ. SpoIIID itself also regulates *cotE* expression. spoIIQ, which is regulated by  $\sigma^F$ , and  $\sigma^E$  result in the engulfment of the forespore (Driks 1999), leading to a free endospore contained in the mother cell.

After engulfment,  $\sigma^F$  leads to the transcription of  $\sigma^G$ , which in turn leads to the transcription of DNA-binding proteins and small acid-soluble proteins (Driks 1999), which serve some role in endospore resistance (Nicholson et al. 2000) as stated earlier. SpoIVB in the forespore (Driks 1999) cleaves the membrane protein SpoIVFA. SpoIVFA, BofA, and SpoIVFB are membrane proteins which complex and hold SpoIVFB inactive. The cleavage of SpoIVFA frees SpoIVFB, which then activates pro- $\sigma^K$  to  $\sigma^K$  (Dworkin 2014) in the mother cell (Driks 1999).  $\sigma^K$  alone controls the transcription of genes encoding at least 11 spore coat proteins: CotA, CotD, CotF, CotH, CotM, CotT, CotV, CotW, CotX, CotY, and CotZ. It also controls transcription and the transcription factor GerE.  $\sigma^K$  and GerE together regulate the expression of

genes encoding CotB, CotC, CotG, and CotS, as well as CotV, CotW, CotX, CotY, and CotZ (Driks 1999). While these are not all of the genes expressed during sporulation, they will be sufficient to explain the gene expression that controls spore coat formation in *B. subtilis*.

To begin the formation of the spore coat around the forespore, SpoIVA localizes to the outer membrane of the forespore. CotE then localizes to the outer membrane of the forespore as well, forming a ring about 75 nm from the outer membrane (Henriques and Moran 2007). The area between the outer membrane and the ring of CotE, called the precoat (Henriques and Moran 2007) or matrix (Driks 1999), has an unknown makeup (Henriques et al. 2007), though it may contain CotA and CotJ (Driks 1999). Multiple coat proteins, including CotD, CotH, CotS, and CotT localize around the CotE ring, forming the inner coat (Driks 1999). CotE is involved in attaching the inner coat to the endospore surface, and may interact with CotT (Henriques et al. 2007). CotE is also involved in the deposition of proteins to form the outer coat (Henriques et al. 2007), along with CotA, CotM (Driks 1999), CotH, CotO (Henriques et al. 2007), CotC, and CotU (Isticato et al. 2010). CotG and CotB are then deposited in the outer coat (Driks 1999; Figure 4), where CotG is stabilized by CotH (Henriques et al. 2007). The matrix is replaced by peptidoglycan under the control of  $\sigma^K$ , as  $\sigma^K$  controls the transcription of peptidoglycan precursors (Vasudevan et al. 2007). At this point, the *B. subtilis* spore coat is fully formed and can be released from the mother cell via lysis. The spore coat is strengthened by the cross-linking enzyme Tgl, which acts on the protein GerQ (Kim et al. 2006), and possibly on other polypeptides (Henriques and Moran 2007).

CotE in *B. subtilis*. The protein CotE plays an important role in the formation of the *B. subtilis* spore coat. While *B. subtilis* endospores that lack CotE still construct an inner coat, the inner coat is not firmly attached to the endospore. Instead, the inner coat is not in direct contact with



the cortex and appears swollen and not properly attached to the cortex (Driks 1999; Riesenman and Nicholson 2000). This is likely due to CotE's position at the junction of the cortex and inner coat (Driks 2002) suggesting a role in attaching the inner coat to the endospore surface (Henriques and Moran 2007). In contrast to the inner coat, CotE mutants do not construct any outer coat (Zheng et al. 1988; Driks 2002). This results from CotE's role in outer coat protein deposition, as it interacts with at least 13 coat proteins involved in the outer coat (Kim et al. 2006).

These structural effects of lacking CotE understandably lead to changes in the endospore's resistance. *CotE* mutants were much more affected by lysozyme, an enzyme which can damage the structure of bacterial cell walls (Smolelis and Harsell 1949), lysing when exposed to the enzyme. After approximately 10 minutes of exposure to lysozyme, the density of a culture containing *cotE* mutants was only about 35% of the initial density, indicating that approximately 65% of the mutants were lysed by the lysozyme. In contrast, a culture of wildtype *B. subtilis* endospores showed almost no decrease in density, corresponding to almost no endospores being lysed (Zheng et al. 1988). *CotE* mutants were also much more sensitive to sodium hypochlorite, with a survival rate of about 60% after only two minutes of exposure. In contrast, wildtype endospores showed practically no decrease in survival over the same time interval (Ghosh et al. 2008). Likewise, *cotE* mutants were significantly more sensitive to hydrogen peroxide, with only about a fifth as many mutants as wildtype endospores surviving exposure (Riesenman and Nicholson 2000). These results would suggest that an endospore's lysozyme, bleach, and hydrogen peroxide resistances are due to either the outer coat or the attachment of the inner coat to the endospore, as those are the two physiological effects of CotE absence (Driks 1999; Zheng et al. 1988).

*CotE* mutant endospores are just as resistant as wildtype endospores to moist heat (Ghosh et al. 2008) and chloroform exposure (Zheng et al. 1988), which would seem to indicate that resistance to these pressures is not directly due to the outer coat or the attachment of the inner coat to the endospore. Instead, the resistance may arise from the inner coat, or from other non-coat properties such as low core water content, the mineral content of the endospore, or the presence of  $\alpha/\beta$ -Type small acid-soluble proteins (SASP).

Interestingly, *cotE* mutants were significantly more resistant to UV-A, UV-B, UV-A+B, and UV-C exposure than their wildtype counterparts. The reason for this increased resistance is unknown, as *cotE* mutants are lacking an outer coat and have a malformed inner coat, which would seemingly indicate that they are less protected from exposure to environmental factors (Riesenmann 2000).

Other Coat Genes in *B. subtilis*. CotE's large effect on morphogenesis and resistance is not typical of the loss of a single coat protein. For example, CotA mutant endospores lack the brown pigmentation found in wildtype endospores, while CotD mutants germinate more slowly than wildtype endospores (Donovan et al. 1987). However, neither mutant showed any significant phenotypical effects. CotH mutation leads to a thinner outer coat and less closely associated inner and outer coats (Zilhao et al. 1999). While these mutants germinated less efficiently than wildtype endospores, they were just as resistant to heat, lysozyme, and chloroform as were wildtype endospores (Naclerio et al. 1996). Together, these effects suggest that the morphogenic role of CotE is much more significant than the morphogenic role of most other coat proteins, such as CotA and CotD in multiple species of *Bacilli*.

*B. anthracis* Sporulation. The formation of the *B. anthracis* spore coat is similar to the formation of the *B. subtilis* spore coat. For example, sigma factors are expressed in the same order in *B.*

*anthracis* sporulation as they are in *B. subtilis* sporulation (Liu et al. 2004). This is not surprising, as the vast majority of sporulation genes that are found in *B. subtilis* are either very similar or have regions of similarity to genes found in *B. anthracis* (Onyenwoke et al. 2004). However, there are some notable differences between the spore coat formation of *B. anthracis* and that of *B. subtilis*. *B. anthracis* produces an exosporium around its spore coat. The formation of the exosporium involves at least 137 different proteins, at least 21 of which are unique to the exosporium (Liu et al. 2004). The protein ExsY is necessary for formation of the endospore, as *ExsY* mutants form an incomplete exosporium, if they form one at all. The incomplete exosporium arrests as a and covers only one end of the endospore. This “cap” has an abnormal inner layer, though the outside appears unaltered (Boydston et al. 2006). Though not as significant as ExsY’s role, the protein ExsM plays an important role in the formation of the exosporium. In *B. anthracis ExsM* mutants, the exospore was not properly attached to the spore coat. Interestingly, a fraction of the mutants also showed a partial second exosporium, possibly due to overcompensation of a related protein in ExsM’s absence (Fazzini et al. 2010).

CotE in *B. anthracis*. While CotE plays a significant role in *B. subtilis* endospore formation (Driks 2002; Henriques and Moran 2007), it plays a more minor role in *B. anthracis* spore coat formation. *B. anthracis cotE* mutants still produced both an inner and outer spore coat, though these coats were not properly attached to the cortex (Giorno et al. 2007). This contrasts with *B. subtilis cotE* mutants which entirely lacked an outer spore coat (Zheng et al. 1988). However, *B. anthracis cotE* mutants did lack a complete exosporium, as it was fragmented or not formed at all (Giorno et al. 2007). CotE is not found in the exosporium itself, but is in the coat (Giorno et al. 2007), as in *B. subtilis* (Driks 2002), as well as in the interspace (Giorno et al. 2007). Thus,

the malformed exosporium is likely due to the inability for it to properly attach to the outer spore coat, and not due to impaired synthesis of the exosporium itself (Giorno et al. 2007).

Despite these somewhat significant physiological differences, *B. anthracis cotE* mutants only fail to express a single protein that is expressed in wildtype *B. anthracis* (Giorno et al. 2007). In contrast, *B. subtilis cotE* mutants fail to fully express at least five different coat proteins in the spore coat, which leads to increased sensitivity to lysozyme (Zheng et al. 1988). This increased lysozyme sensitivity is not found in *B. anthracis cotE* mutants. The *B. anthracis cotE* mutants are also fully virulent in intramuscular and intranasal models (Giorno et al. 2007). These results suggest that the exosporium is not required for lysozyme resistance or virulence in *B. anthracis*.

Other Coat Genes in *B. anthracis*. *B. anthracis cotH* mutants showed minimal physiological differences as compared to wildtype endospores, only having a reduced number of ridges in the spore coat. CotH mutant endospores were slightly altered late in germination, resulting in a larger number of germinating endospores. Despite these small changes, *B. anthracis cotH* mutants were fully virulent (Giorno et al. 2007). Notably, CotH in *B. anthracis* did not seem to act with CotE (Giorno et al. 2007) as it does in *B. subtilis* (Driks 1999).

CotE in *Bacillus cereus*. Hinting at the possible conservation of the role of CotE, CotE mutants of *Bacillus cereus*, which is less related to *B. anthracis* and *B. subtilis* than they are to each other, also showed major morphological changes. Unlike *B. subtilis*, *B. cereus* produces an exosporium in addition to its spore coat. *B. cereus cotE* mutants had a malformed exosporium which was fragmented in places and not properly attached to the outer spore coat. *cotE* did not produce detectable levels of 19 proteins which were detected in wildtype *B. cereus* endospores. These morphological changes and changes in expression led to endospores that were significantly less

hydrophobic than their wildtype counterparts. Additionally, the endospores were significantly less resistant to UV-C, hydrogen peroxide, and lysozyme than wildtype endospores were (Bressuire-Isoard et al. 2016). These major morphological changes caused by the absence of CotE again point to the central role played by CotE in spore coat formation.

**Spore Coat as A Model System.** As the roles of the genes and proteins involved in spore coat formation have been well elucidated, the spore coat has been proposed as a model system for studying other complex structures (Driks 1999; Driks 2004). Previous studies have used varying methods in order to study a particular gene's role in the formation and regulation of the bacterial spore coat. In one study, gene fragments were inserted into vectors which were then taken up by transformed *B. subtilis*, interrupting the gene of interest after a double crossing-over event (Beall et al. 1993). Another study used linear DNA to create an insertion-deletion event in the gene of interest, effectively knocking out the gene after transformation and double recombination into *B. subtilis* (Zheng et al. 1988). A third study amplified multiple fragments from the gene of interest and inserted two fragments into a plasmid containing antibiotic resistance genes, which was subsequently amplified using *E. coli*. *B. anthracis* which had integrated the plasmid were selected for, and a second crossing-over event led to knocking out of the gene of interest. This was confirmed via PCR analysis (Shatalin and Neyfakh 2005). More recently, multiple fragments of a gene of interest were amplified and ligated together, then inserted into a plasmid backbone. After amplification by *E. coli*, *B. cereus* was transformed and a double crossing-over event was induced, deleting the gene of interest (Bressuire-Isoard et al. 2016).

In this study, another method for studying the role of a single gene in spore coat formation is developed. A single amplified fragment of the *B. anthracis cotE* gene can be inserted into a preexisting plasmid backbone, containing an antibiotic resistance gene, after both

are digested with the same restriction enzymes. This plasmid can then be selected for using antibiotic media, amplified by *E. coli*, and the correct insert can be confirmed via restriction digests. *B. anthracis* can be transformed with the plasmid, which can then integrate into the bacterial genome via homologous recombination and a crossing-over event, resulting in an insertion-deletion event in the *cotE* gene. The effect of this insertion-deletion can then be studied. As many species of *Bacilli* have not yet been sequenced, a plasmid containing a fragment of their specific *cotE* sequence cannot be developed. However, the relatively high conservation of *cotE* across species of *Bacilli* (Onyenwoke 2004) should allow other species to be transformed with the plasmid and for homologous recombination and an insertion-deletion event to occur as in *B. anthracis*.

The development of this plasmid could assist in determining the morphogenic role of CotE in multiple species of *Bacilli* which have not been closely studied, and may allow for the detection of patterns in the role of CotE across different species of *Bacilli*. Success in this could present this method of research as a viable option for studying the bacterial spore coat, and more importantly, can be applied to studying complex structures in general.

This work builds off of a previously created plasmid, pNCCH1 (Figure 5A). The pNCC backbone contains an origin of replication, a kanamycin resistance gene, an erythromycin resistance gene, and the *B. anthracis cotH* gene flanked by PstI and NotI restriction sites. The origin is temperature sensitive and replicates well at 30°C, but only replicates well at 37°C if it is integrated into the bacterial chromosome.

## **EXPERIMENTAL PROCEDURES**

**Conservation Analysis.** The *cotE* sequences for 17 bacteria of the genus *Bacillus* (*B. anthracis* str. Sterne, *B. subtilis*, *B. cytotoxicus*, *B. weihenstephanensis*, *B. cereus*, *B. megaterium*, *B. pumilus*, *B. atropthaeus*, *B. thuringiensis*, *B. cellulosilyticus*, *B. clausii*, *B. coagulans*, *B. halodurans*, *B. licheniformis*, *B. pseudofirmus*, *B. toyonensis*, and *B. amyloliquefaciens*) and 1 of the genus *Oceanobacillus* (*O. iheyensis*) were downloaded from NCBI (NCBI Resource Coordinators 2016). The sequences were then aligned using CLUSTALW (*CLUSTALW*) and viewed using Jalview (Waterhouse et al. 2009). A phylogenetic tree was also constructed using the neighbor joining method in Jalview (Waterhouse et al. 2009) in order visualize the conservation of *cotE*.

**Design of Primers.** Using the alignment, the most conserved region was identified. Since PstI and NotI were required in order to excise *cotH* from pNCCH1, NEBcutter V2.0 (Vincze et al. 2003) was used to ensure that there were no PstI or NotI restriction sites in the *cotE* sequence. The Saccharomyces Genome Database Web Primer tool (*Web Primer*) was used to determine the optimal forward primer and reverse primer. A PstI restriction site was then added to the forward primer and a NotI restriction site was added to the reverse primer.

**Amplification of *cotE* Fragment.** Previously isolated *B. anthracis* str. Sterne DNA, the forward and reverse primers, and PuReTaq Ready-To-Go PCR Beads (GE Healthcare Life Sciences) were used to amplify the *cotE* fragment via PCR with the following conditions:

1. 94°C for 5 minutes
2. 94°C for 30 seconds
3. 65°C for 30 seconds
4. 72°C for 45 seconds
5. Repeat 2-5 for 59 more cycles

6. 72°C for 5 minutes

The amplification was confirmed by running the PCR product with EZ-Vision (AMRESCO) on an agarose gel and viewing under UV light. The *cotE* fragment was then excised and purified using the Zymoclean™ Gel DNA Recovery Kit (Zymo Research) following the included protocol (Zymo Research, *Instruction Manual: Zymoclean™*).

**Restriction Digest of *cotE* Fragment and pNCCH1.** The plasmid pNCCH1, containing a *cotH* fragment flanked by a NotI restriction site and a PstI restriction site, was previously constructed (Peterson). The pNCC backbone contained kanamycin resistance, restriction sites, and an origin of replication.

The *cotE* fragment was digested by NotI and PstI-HF (New England BioLabs) at 37°C for an hour in order to create sticky ends. The digest product with EZ-Vision (AMRESCO) was then separated via gel electrophoresis and viewed under UV light to confirm the presence of *cotE*. The digested *cotE* fragment was purified using Zymoclean™ Gel DNA Recovery Kit (Zymo Research) following the included protocol (Zymo Research, *Instruction Manual: Zymoclean™*). pNCCH1 was digested by NotI and PstI-HF in order to excise the *cotH* fragment from the pNCC backbone. The product with EZ-Vision (AMRESCO) was separated via gel electrophoresis on a 1% agarose gel and viewed under UV light, and the putative pNCC backbone was excised and purified using Zymoclean™ Gel DNA Recovery Kit (Zymo Research) following the included protocol (Zymo Research, *Instruction Manual: Zymoclean™*). Both digests were done in duplicate.

**Ligation of *cotE* Fragment into pNCC Backbone.** The digested *cotE* fragment and the digested pNCC backbone were ligated following the New England BioLabs sticky end ligation protocol (New England BioLabs). Additional incubation time was added, for 1 hour of incubation total.



**Transformation of TAM1 Competent *E. coli*.** Competent TAM1 *E. coli* cells (New England BioLabs) were transformed with the putative pNCCE1 plasmid following the Active Motif Protocol (Active Motif RapidTrans 2012). After transformation, the cells were incubated at 30° C instead of 37° C.

The transformed cells and negative control untransformed cells were each plated on three different plates. Lysogeny broth (LB) + 50 µg/mL plates were used to select for cells carrying kanamycin resistance and an LB plate was used as a control.

**Growth of and DNA Isolation from Minipreps.** A single colony that grew on a kanamycin plate was added to a flask of liquid LB + kanamycin and grown at 30° C with shaking. This was repeated for four colonies that showed kanamycin resistance.

Plasmid DNA was isolated from each culture using the Zyppy™ Plasmid Miniprep Kit (Zymo Research), following the kit protocol (Zymo Research, *Instruction Manual: Zyppy™*). *E. coli* cells were pelleted, resuspended, and lysed. Non-plasmid DNA was precipitated out and the remaining plasmid DNA was washed (Zymo Research, *Instruction Manual: Zyppy™*).

**Restriction Digests of Miniprep DNA.** Plasmid DN isolated from each miniprep was subjected to four different restriction digests: an *Ava*II digest, a *Bam*HI digest, an *Eco*RV digest, and a *Not*I & *Pst*I-HF digest (New England BioLabs). The digests were performed following the NEBcloner Restriction Digest Protocol for the appropriate restriction enzyme(s) (*NEB Cloner: RE Digest*). Each isolation also had a control without any restriction enzymes. The digests and undigested negative controls were stained with EZ-Vision (AMRESCO) and then separated via gel electrophoresis and viewed under UV light, where the actual fragment sizes were compared to the expected fragment sizes. Expected fragment sizes for pNCCE1, pNCCE1, and the pNCC

backbone for each restriction digest were determined using NEBCutter V2.0 (Vincze et al. 2003).

**Growth of and DNA Isolation from Midiprep.** Minipreps that appeared to contain the desired pNCCE1, as indicated by the miniprep restriction digests, were transferred to larger flasks of liquid LB +kanamycin and grown in a 30° C shaker. The midiprep plasmid DNA was isolated using the QIAGEN Plasmid Midi Kid (QIAGEN) following the kit protocol (QIAGEN 2012).

**Restriction Digests of Midiprep DNA.** Each midiprep isolation had a control with no restriction digests, as well as an *Ava*II digest, a *Bam*HI digest, an *Eco*RV digest, and a *Pst*I & *Not*I digest. The digests were performed following the NEBcloner Restriction Digest Protocol for the appropriate restriction enzyme(s) (*NEB Cloner: RE Digest*). However, the enzyme concentration was doubled. The digests with EZ-Vision (AMRESCO) were then separated via gel electrophoresis and viewed under UV light, where the actual fragment sizes were compared to the expected fragment sizes. Expected fragment sizes for pNCCE1, pNCCE1, and the pNCC backbone for each restriction digest were determined using NEBCutter V2.0 (Vincze et al. 2003).

## RESULTS

**Conservation Analysis.** *CotE* sequences for 17 species of *Bacilli* and 1 species of *Oceanobacillus* were aligned using CLUSTALW (*CLUSTALW*) and viewed with Jalview (Waterhouse et al. 2009; Figure ). A phylogenetic tree was constructed using the aligned sequences (Figure ).

**Design of Primers.** The most conserved region of *cotE* was identified (Figure 6). This corresponds to the 98-433 bp segment of the coding region of the *B. anthracis cotE* gene. The

optimal primers were determined using the Saccharomyces Genome Database Web Primer tool (*Web Primer*). The forward primer has 6 additional bases and a PstI recognition sequence, followed by 21 bases (bp 98-118) complementary to the *B. anthracis cotE* sequence. The reverse primer has 6 additional bases and a NotI restriction sequence, followed by 21 bases (bp 413-433) that are the inverse complement to the *B. anthracis cotE* gene (Table 1). The total length of the expected fragment amplified with the primers is 362 bp.

**Amplification of *cotE* Fragment.** The primers were used with previously isolated *B. anthracis* Sterne strain genomic DNA in order to amplify the appropriate region of *cotE* via PCR. The *cotE* fragment PCR product and a negative control PCR product with no genomic DNA were both separated by gel electrophoresis and viewed under UV light to determine fragment size. The *cotE* fragment band appeared to be ~400 bp in length (Figure 8), which agreed with the expected amplified fragment size of 362 bp.

The *cotE* fragment was excised from the gel (Figure 9) and purified.

**Restriction Digest of *cotE* Fragment and pNCCH1.** The *cotE* fragment was double digested by PstI and NotI (New England BioLabs) in order to form a fragment with sticky ends. The digest product was then separated via gel electrophoresis and viewed under UV light (Figure 10A) to confirm the presence of the fragment. The product appeared to be ~500 bp in length (Figure 10A), slightly larger than the expected ~350 bp. The products was then excised (Figure 11A) and purified.

pNCCH1 was double digested by PstI and NotI (New England BioLabs) in order to excise the *cotH* fragment from the pNCC backbone, leaving the pNCC backbone with sticky ends complimentary to the digested *cotE* fragment. The digest product was ran in agarose gel and viewed under UV light (Figure 10B) to identify the desired pNCC backbone fragment. The

digest produced a band at ~6,000 bp, which corresponded the uncut pNCCH. The pNCC backbone appeared at ~5,000 bp as expected (Figure 10B). There was no clear band at ~700 bp which would have been expected from the excised 669 bp *cotH* insert, likely due to the small amount of *cotH* excised.

**Ligation of *cotE* Fragment into pNCC Backbone.** The digested *cotE* fragment and the digested pNCC backbone were ligated with the intention form pNCCE1 – a plasmid containing the pNCC backbone and the *cotE* fragment.

**Transformation of TAM1 Competent *E. coli*.** Competent TAM1 *E. coli* cells were transformed with the putative pNCCE1. These cells were then plated on three different plates: 50 µl of cells on LB + Kan, 100 µl of cells on LB + Kan, and the remainder of the cells on LB. Both Kan plates showed scattered growth (~25 colonies on the 50 µl plate, ~35 colonies on the 100 µl plate; Figure 12A), indicating that some cells were successfully transformed with the pNCC backbone which contained a kanamycin resistance gene. The LB plate had a lawn of growth (Figure 12A).

A negative control using untransformed TAM1 *E. coli* cells was plated in the same manner. Neither Kan plate had any growth, indicating that the cells did not have kanamycin resistance, as expected. The LB plate had a lawn of growth, showing that the cells were viable (Figure 12B).

**Growth of and DNA Isolation from Minipreps.** Four different cultures were grown in LB + kanamycin broth, each from a different transformed colony showing kanamycin resistance. DNA was then isolated from each culture.

**Restriction Digests of Miniprep DNA.** Each of the four miniprep products was identified by running four different restriction digests: an *Ava*II digest, a *Bam*HI digest, a *Eco*RV digest, and a

PstI and NotI digest, for sixteen restriction digests in total. Each miniprep product also had an undigested negative control. The fragments produced by the sixteen digests and four negative controls were separated via gel electrophoresis and viewed under UV light (Figure 13). The fragment sizes for each digest were compared to the expected fragment sizes (Table 2).

Digestion of pNCCE1 with AvaII should result in fragments of 70, 453, 624, and 4259 bp in length (Table ). Miniprep 1 resulted in a band at ~750 bp (Figure , Lane 1B), which was not expected with pNCCE1. However, pNCCH1 would result in a 783 bp fragment (Table ), and thus miniprep 1 appeared to contain pNCCH1. It also resulted in a band above 5000 bp corresponding to uncut plasmid DNA. Miniprep 2 resulted in bands at ~650 and ~750 bp (Figure , Land 2B), which were again not indicative of pNCCE1. These bands seemed to correlate to the 624 and 783 bp fragments expected to result from pNCCH1 (Table ). It also resulted in a band above 5000 bp corresponding to uncut plasmid DNA. Miniprep 3 resulted in a band ~4500 bp (Figure , Lane 3B), but each digest was expected to result in a 4259 bp fragment (Table ) and thus this band was not indicative of a specific plasmid. Miniprep 4 resulted in a band at ~600 bp but none at ~750 bp (Figure , Lane 4B), which would indicate that it contained either pNCCE1 or the pNCC backbone. However, it did not result in a band at 453 bp as expected from a pNCCE1 digest or at 103 bp as expected from a pNCC backbone digest (Table ).

It also produced the nonspecific band ~4500 bp (Figure , Lane 4B).

Digestion of pNCCE1 with BamHI should result in a 1138 bp and a 4268 bp fragment (Table ). Miniprep 1 resulted in a band above 5000 bp due to uncut plasmid DNA and a nonspecific band ~1100 (Figure , Lane 1C) which corresponds to the 1138 bp fragment expected from each possible plasmid (Table ). Miniprep 2 also resulted in a band above 5000 bp due to uncut plasmid and a nonspecific band at ~1100 bp (Figure , Lane 2C). Miniprep 3 resulted in

band ~4000 bp (Figure , Lane 3C), which could correspond to the 4268 bp band expected from a pNCCE1 digest, the 4034 bp band expected from a pNCCH1 digest, or 3918 bp band expected from a pNCC backbone digest (Table ). Due to the similar lengths of these fragments, the exact identity of the ~4000 bp band could not be determined. Miniprep 4 produced both a band above 5000 bp due to uncut plasmid DNA and the nonspecific ~4000 bp band (Figure , Lane 4C).

An EcoRV digest of pNCCE1 should result in a 1025 bp fragment and a 4381 bp fragment (Table ). Miniprep 1 resulted in a band above 5000 bp from uncut plasmid DNA and a band ~1000 bp (Figure , Lane 2D). While a 1025 bp fragment would result from a pNCCE1 digest, it would also result from a pNCCH1 or a pNCC backbone digest (Table ), and thus this band was inconclusive. Miniprep 2 also resulted in band above 5000 bp from uncut plasmid DNA and the nonspecific band at ~1000 bp (Figure , Lane 2D). Miniprep 4 resulted in a band at ~4500 bp (Figure , Lane 3D). This could correspond to the 4381 bp fragment expected from a pNCCE1 digest or the 4496 bp fragment expected from a pNCCH1 digest (Table ). It also resulted in the nonspecific band at ~1100 bp (Figure , Lane 3D). Miniprep 4 resulted in the nonspecific band at ~4500 bp (Figure , Lane 4D).

A double digest using PstI and NotI of pNCCE1 should result in a 339 bp fragment and a 5067 bp fragment (Table ). Miniprep 1 only resulted in a band above 5000 bp due to uncut plasmid DNA (Figure , Lane 1E). Miniprep 2 produced a band at ~5000 bp (Figure , Lane 2E), which could be due to the 5067 band that would result from a digest of pNCCE1 or of pNCCH1 or the 5056 band that would result from a digest of the pNCC backbone (Table ). However, it also produced a band ~650 bp (Figure , Lane 3E), which corresponds to the 669 bp band expected from a pNCCH1 digest (Table ). Thus, miniprep 2 appeared to contain pNCCH1.

Miniprep 3 only produced a band above 5000 bp due to uncut plasmid DNA (Figure , Lane 3E). Miniprep 4 resulted in the nonspecific band at ~5000 bp (Figure , Lane 4E).

In summary, the ~750 bp fragment from the *Ava*II digest of miniprep 1 (Figure , Lane 1B) corresponded to the 783 bp fragment expected from a digest of pNCCH1 (Table ). Miniprep 1 likely contained pNCCH1. The *Ava*II digest of miniprep 2 resulted in bands ~650 bp and ~750 bp (Figure , Lane 2B), which correspond to the 624 bp and 783 bp fragments expected from a digest of pNCCH1 (Table ). The *Pst*I and *Not*I double digest of miniprep 2 resulted in a band at ~650 bp (Figure , Lane 2E), corresponding to the 669 bp fragment expected from a pNCCH1 digest (Table ). Thus miniprep 2 also appeared to contain pNCCH1. None of the restriction digests of miniprep 3 produced bands indicative of any specific plasmid, and therefore the plasmid DNA isolated from miniprep 3 was not conclusively identified. The *Ava*II digest of miniprep 4 resulted in a band at ~600 bp but none at ~750 bp (Figure , Lane 4B), which corresponded to the 624 bp band expected from either pNCCE1 or the pNCC backbone (Table ). Miniprep 4 therefore seemed to contain pNCCE1 or the pNCC backbone.

**Growth of and DNA Isolation from Midiprep.** Miniprep 4 seemed to contain pNCCE1 or the pNCC backbone, and thus a midiprep culture was prepared from the miniprep. Miniprep 3 did not produce any conclusive results, so a midiprep culture was prepared from the miniprep in order to test further.

After allowing to incubate, DNA was isolated from each midiprep.

**Restriction Digests of Midiprep DNA.** Both of the midiprep products were identified by running four different restriction digests, for eight restriction digests in total. Each miniprep product also had an undigested negative control. The fragments produced by the eight digests

and two negative controls were separated via gel electrophoresis and viewed under UV light (Figure).

## DISCUSSION

While there are still questions regarding the spore coat formation in *Bacillus*, the spore coat has been proposed as a model system for studying complex systems (Driks 1999; Driks 2004). As complex systems, such as bacterial spore coats, rely on a complex network of genes and proteins, elucidating the role of a single gene and its corresponding protein can prove to be difficult. Multiple methods have been used to study the role of a single gene/protein pair in bacterial spore coats. These details of these methods vary, but all rely on the use of a plasmid containing one or multiple gene fragments interrupting the gene of interest via crossing-over (Beall 1993; Zheng 1988; Shatalin 2005; Bressuire-Isoard 2016).

In this study, development began on a method to study a gene/protein pair's role in the spore coat of less studied species of *Bacilli*, with the goal to show it as a viable method for studying complex structures. The proposed method involved amplification of a single fragment of the *B. anthracis cotE* gene and subsequent ligation into a preexisting plasmid backbone containing an antibiotic resistance gene. *E. coli* transformed with the plasmid of interest could be selected for using antibiotic media, the amplified plasmid could be isolated from the *E. coli*, and the correct insert could be identified via restriction digests. Once the correct plasmid is confirmed, *B. anthracis* can be transformed with the plasmid. Homologous recombination and a double crossing-over event would result in an insertion-deletion event in the genomic *cotE* gene, allowing its function and role in spore coat structure to be studied in species of *Bacilli*. As *cotE* is fairly conserved across sporulating species of *Bacilli*, the same plasmid could be used to study



the role of CotE in multiple species of *Bacilli*, presenting this as a viable method for studying both the bacterial spore coat and complex structures in general.

Primers were successfully designed to flank a highly conserved region of the *B. anthracis* *cotE* gene (Figure) and had restriction sites (Table ) corresponding to restriction sites on the plasmid backbone. The primers were used to amplify a fragment of the correct length PCR, and the fragment's length was confirmed via gel electrophoresis (Figure, Lane 1). However, the fragment was not sequenced and thus its exact identity is not known. Both the *cotE* fragment and the preexisting plasmid were digested with PstI and NotI. This excised the *cotH* fragment from the plasmid backbone and created complimentary sticky ends on the *cotE* fragment and the plasmid backbone. The resulting *cotE* fragment and plasmid backbone were ligated together. TAM1 *E. coli* cells were successfully transformed with the putative plasmid, as indicated by their antibiotic resistant properties (Figure). The plasmid DNA contained in the *E. coli* was successfully isolated. Minipreps 1 and 2 did not appear to contain the desired pNCCE1 plasmid, likely due to contamination by the *cotH* fragment when excising the pNCC backbone from the gel. The bands produced by the restriction digests of miniprep 1 and miniprep 2 agreed with bands that would be expected from pNCCH1 (Figure; Table ), supporting the possibility that there was contamination, likely occurring when the pNCC backbone was excised from the gel (Figure ) for purification.

The identity of plasmid DNA isolated from miniprep 3 was inconclusive (Figure ; Table ) as there were no plasmid-specific fragments produced, and miniprep 4 seemed to contain pNCCE1 or the pNCC backbone (Figure ; Table ). Thus, midipreps were grown from miniprep 3 and miniprep 4 and DNA was isolated from both midiprep 3 and midiprep 4. There were no

bands resulting from the restriction digests of either midiprep, indicating a likely issue in the methodology for plasmid DNA isolation.

While this study provided a starting point for development of this method of study, much work is yet to be done. The procedure for DNA isolation from midipreps must be fixed in order to confirm the identity of the correct plasmid. Alternately, the isolated plasmid DNA could be identified via sequencing. Once it is confirmed that the correct plasmid has been isolated, it should be amplified by *E. coli* to produce a large amount of pNCCE1 available to be used for transformation of *Bacillus* species. *B. anthracis* should be transformed first, as the *cotE* fragment contained in the plasmid should be identical to the corresponding fragment in the *B. anthracis* genome. Thus, integration via homologous recombination can be induced, and a double crossing-over event can result in an insertion-deletion event in the *cotE* gene. The inactivation of the gene can be confirmed via PCR analysis, and the effect of this knock out can be studied. Additional species of *Bacilli*, specifically *B. subtilis*, should also be transformed with pNCCE1, and *cotE* should be knocked out in the same manner.

Should all of these goals be met, the use of a plasmid containing a single gene fragment to knock out the gene can be presented as a practical method for the study of complex structures. This could improve upon the current methods, many of which require multiple gene fragments to be inserted into a plasmid (Beall 1993; Shatalin 2005; Bressuire-Isoard 2016). Thus, the method being developed in this study would provide a simpler way to achieve the same effects, making the study of bacterial spore coats easier. This method could then be extended to the study of complex structures in general, impacting methodology in multiple subdisciplines and assisting the advancement of their studies.

## FIGURES

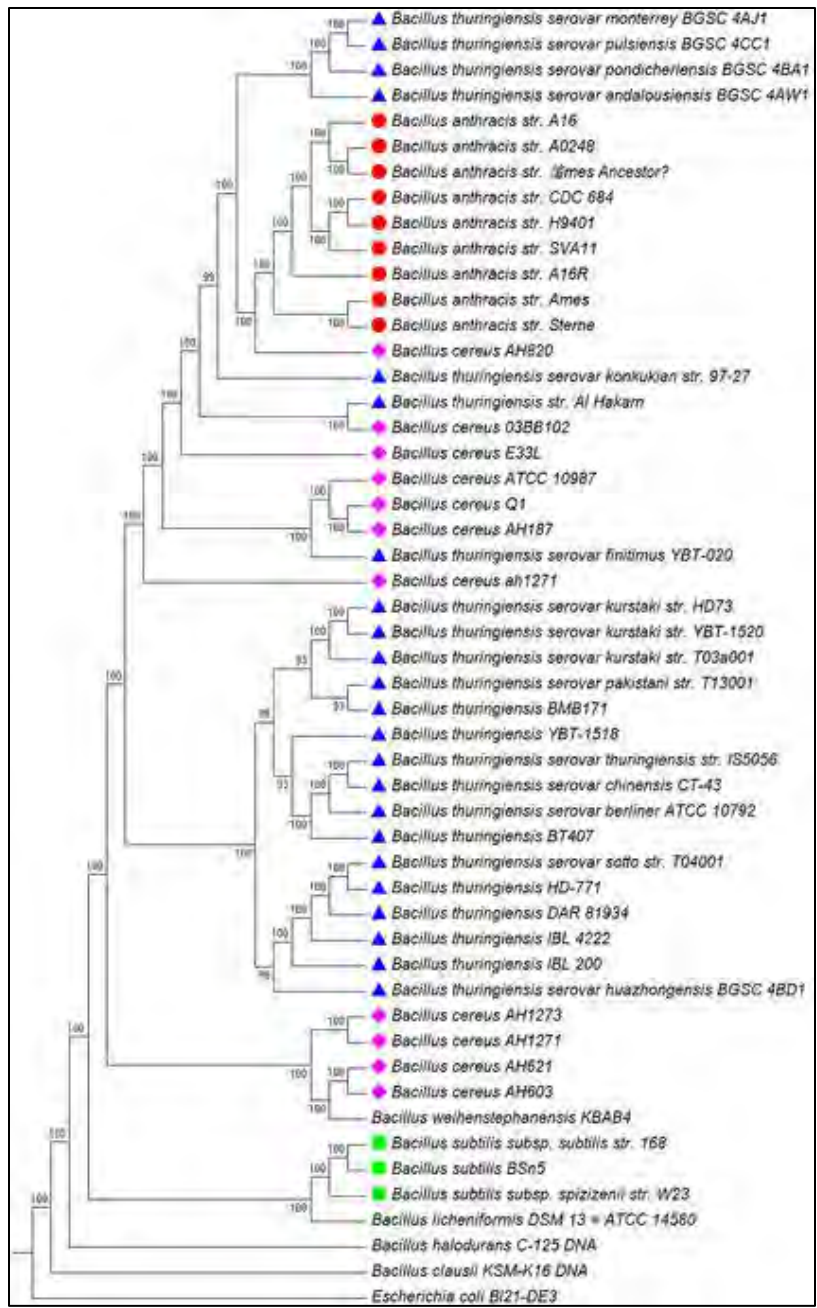


FIGURE 1. **Phylogenetic Tree of *Bacilli* Using Whole Genome Data (Wang and Ash 2015).**

The tree was created using the neighbor joining method and 51 taxa, using *Escherichia coli* as an outgroup.

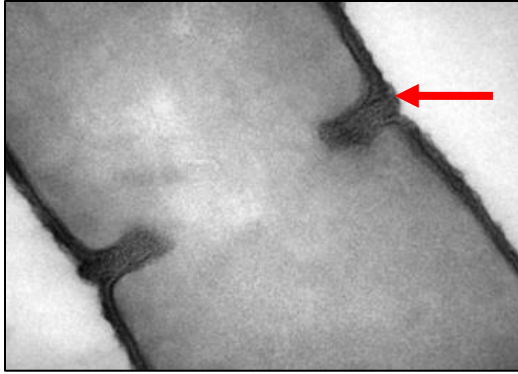


FIGURE 2. *B. subtilis* septum formation (Hyde et al. 2006). Septum indicated by red arrow.

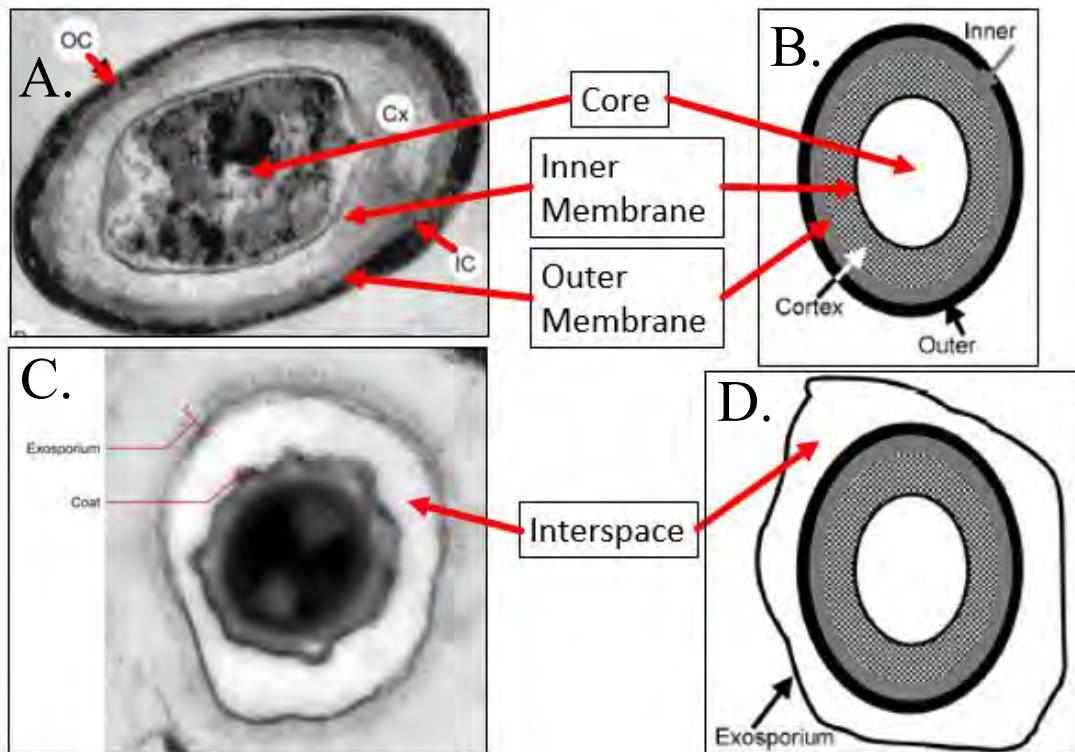


FIGURE 3. **Bacterial Endospore structure.** Endospores of (A) *B. subtilis* (Driks 1999) and (C) *B. anthracis* (Driks 2002), along with general diagrams of bacterial endospores (B) without and (D) with an exosporium (Driks 2004). Major parts of the bacterial spore coat are labeled. OC = Outer coat, IC = Inner coat, Cx = Cortex.

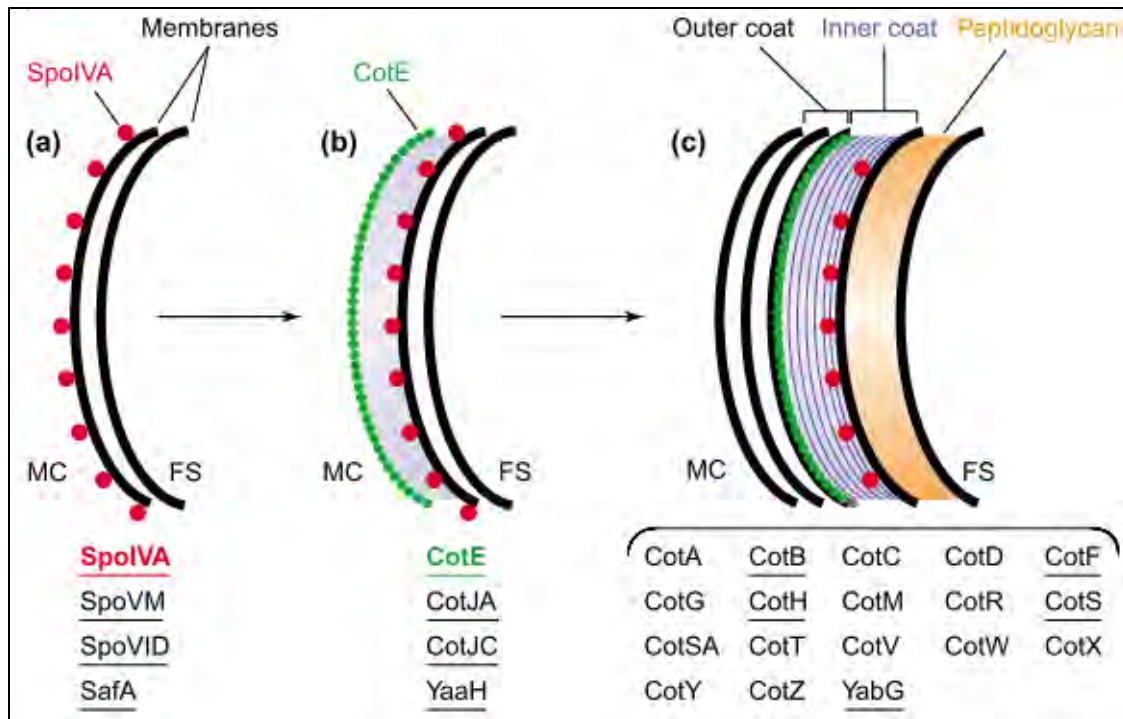
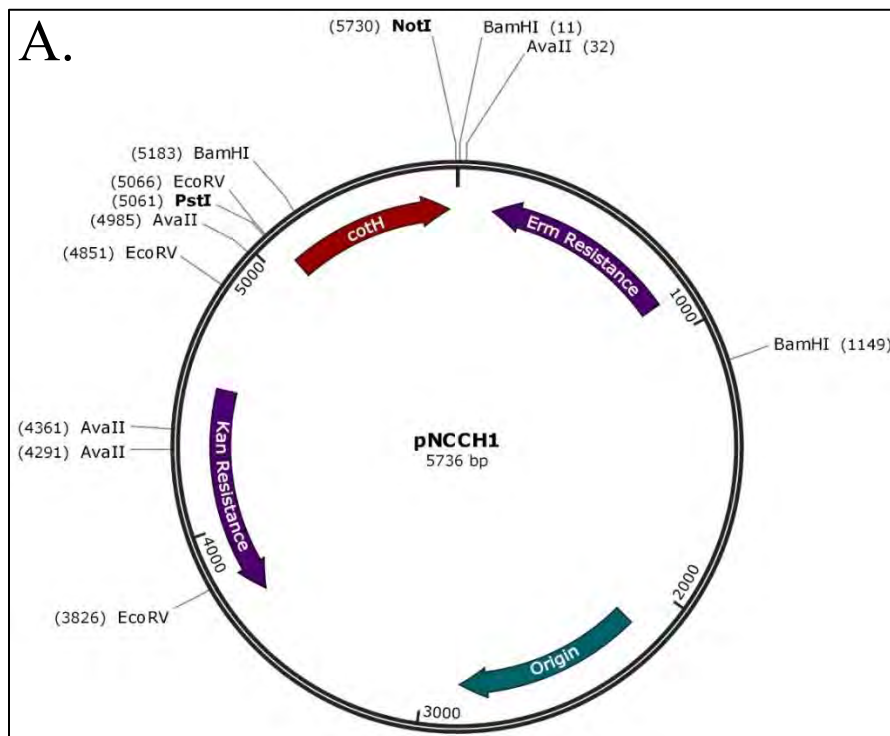


FIGURE 4. **Proteins involved in *B. subtilis* spore coat formation (Driks 2002).** The left side (MC) represents the mother cell, and thus the outside of the endospore. The right side (FS) of the cell represents the forespore, and thus the inside of the endospore.



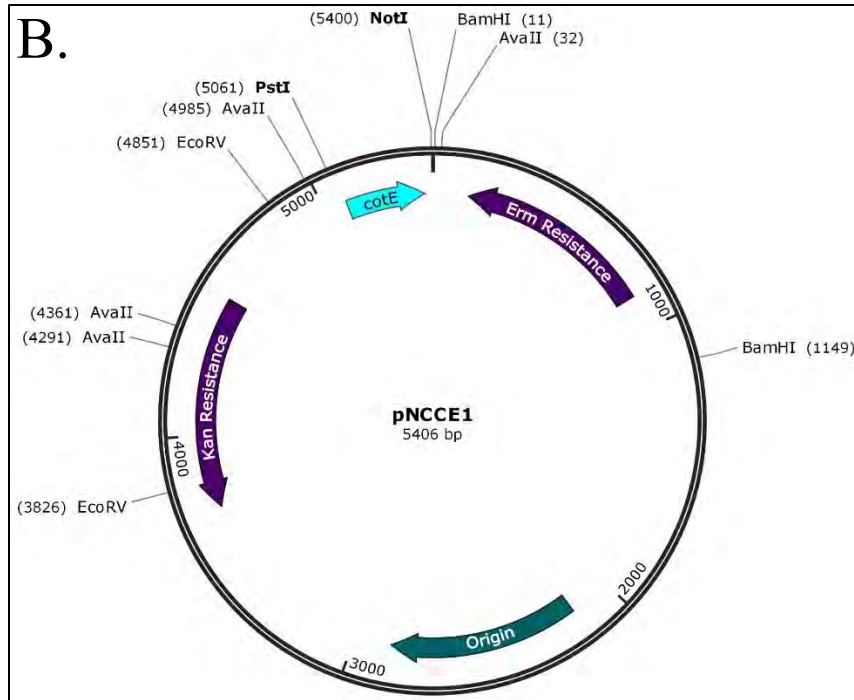


FIGURE 5. **Plasmid maps of (A) pNCCH1 and (B) pNCCE1.** The origin of replication, a kanamycin resistance gene, an erythromycin gene, the PstI restriction site, and NotI restriction site are labeled on both. pNCCH1 contains the *B. anthracis cotH* gene and pNCCE1 contains the *B. anthracis cotE* gene. Maps created using SnapGene (GSL Biotech).



FIGURE 6. **Aligned *Bacillus* and *Oceanobacillus cotE* genes.** Sequences were aligned using CLUSTALW and viewed in JThe darker blue shading corresponds to higher percentage identity among the species aligned. The chosen segment to be amplified (117-461 bp) is marked in red.

TABLE 1. **Primers for *cotE* Amplification.**

Primer	Sequence	Length (bp)
Forward	AAGGAA <b>CTGCAGCAAGTATTTAGGGTGCTGGG</b>	33
Reverse	GGAAGG <b>CGGCCGCCACAATTTTCGTTTCACCAA</b>	35

5' to 3'. PstI recognition sequence in red. NotI recognition sequence in blue. *B. anthracis* genomic DNA in black and bolded. Additional bases in black.

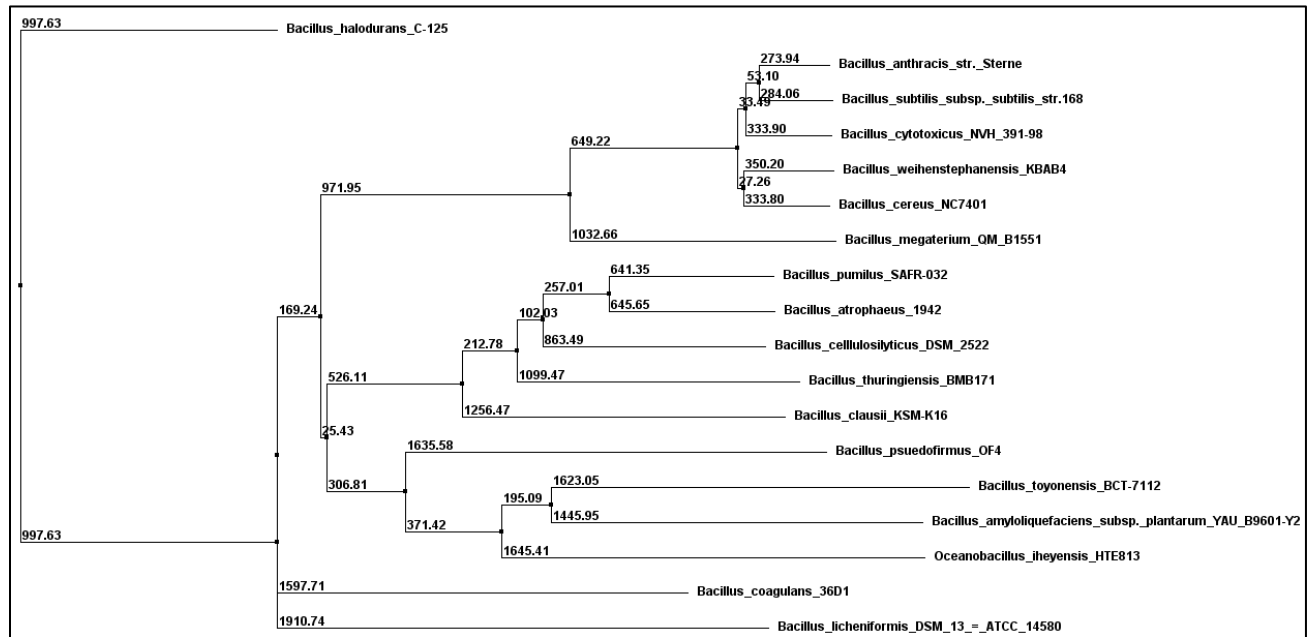


FIGURE 7. **Phylogeny Based on *cotE* Sequences.** The tree was constructed using the neighbor joining method in Jalview (Waterhouse et al. 2009). Distances are denoted at nodes.



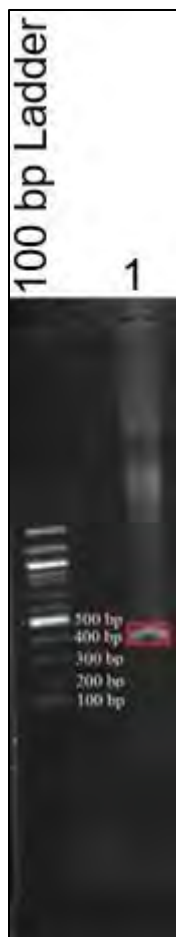


FIGURE 8. ***cotE* Fragment Amplification Product.** PCR product ran with EZ-Vision (AMRESCO) on 1% agarose gel. Lane 1: *cotE* fragment outlined in red, expected length of 362 bp.

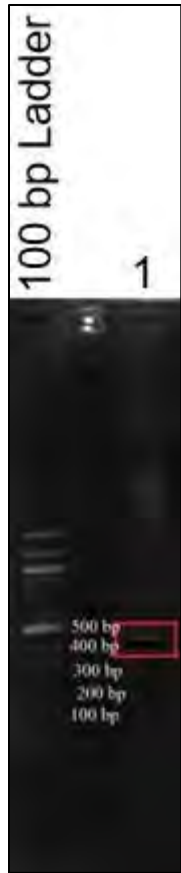


FIGURE 9. **Excised *cotE* Fragment Amplification Product.** Lane 1: Excised *cotE* fragment outlined in red.

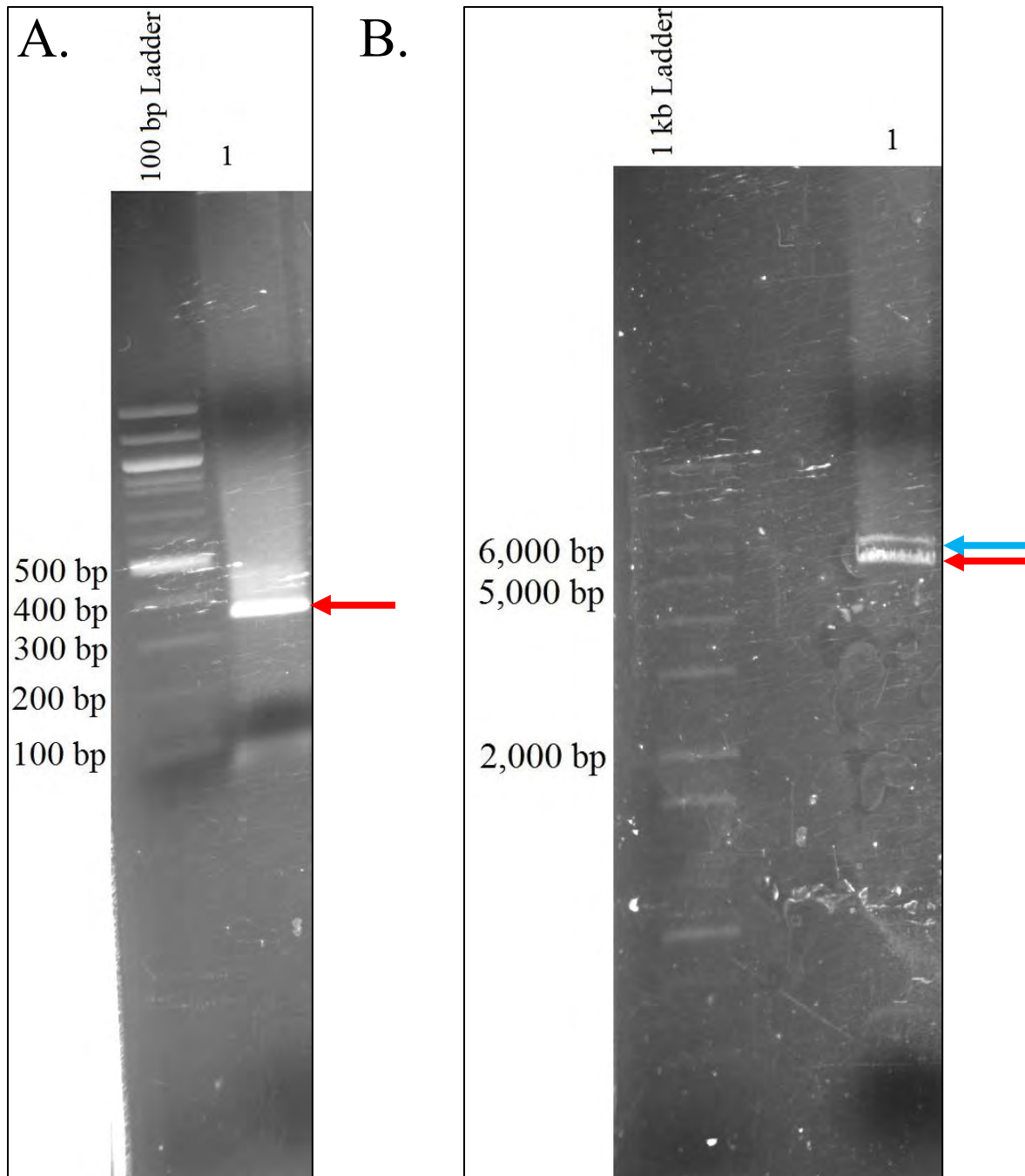


FIGURE 10. *cotE* and pNCCH1 Restriction Digest Products. Restriction digest products ran with EZ-Vision (AMRESCO) on 1% agarose gel. (A) PstI and NotI restriction digest of *cotE* fragment. Lane 1: Digested *cotE* fragment indicated by red arrow. Expected fragment size of 339 bp. (B) PstI and NotI restriction digest of pNCCH1. Lane 1: pNCC backbone without *cotH*

fragment indicated by red arrow. Expected fragment size of 5,067 bp. Uncut pNCCH1 indicated by blue arrow.

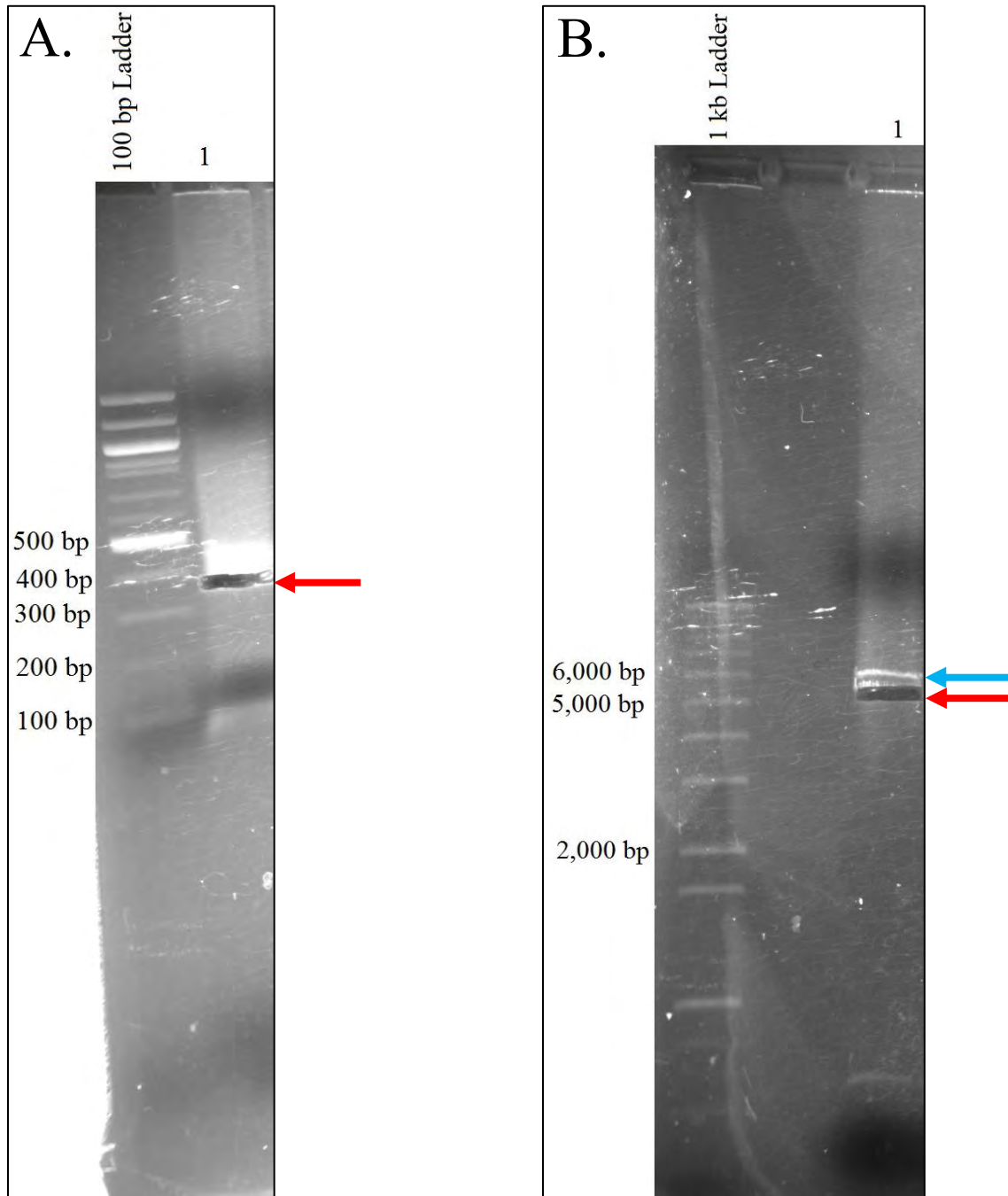


FIGURE 11. *cotE* and pNCCH1 Restriction Digest Products. (A) Excised PstI and NotI restriction digest of *cotE* fragment. Excision indicated by red arrow. (B) Excised PstI and NotI

restriction digest of pNCCH1. Excision of pNCC backbone indicated by red arrow. Uncut pNCCH1, indicated by blue arrow, was not excised.

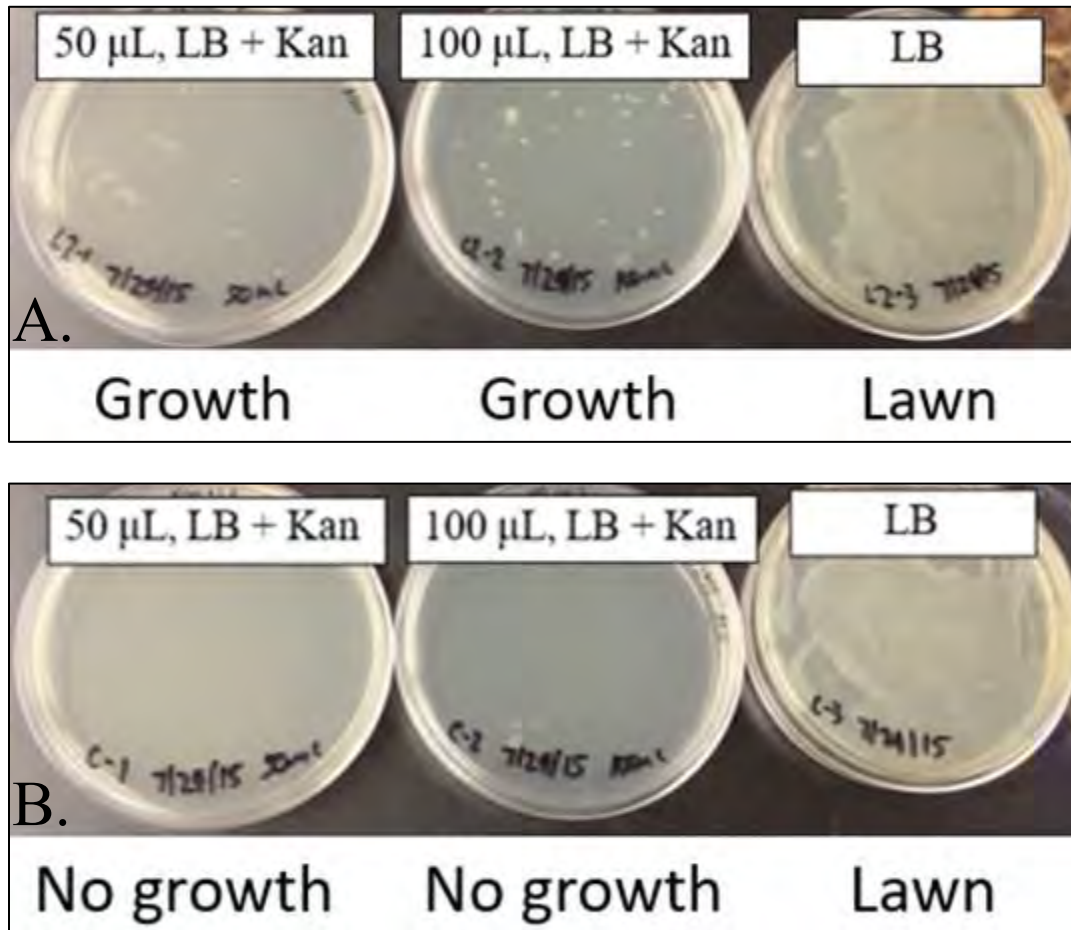


FIGURE 12. **Transformed and Control *E. coli*.** (A) TAM1 *E. coli* transformed with putative pNCCE1. Growth marked under corresponding plate. (B) Untransformed TAM1 *E. coli*. Growth marked under corresponding plate.

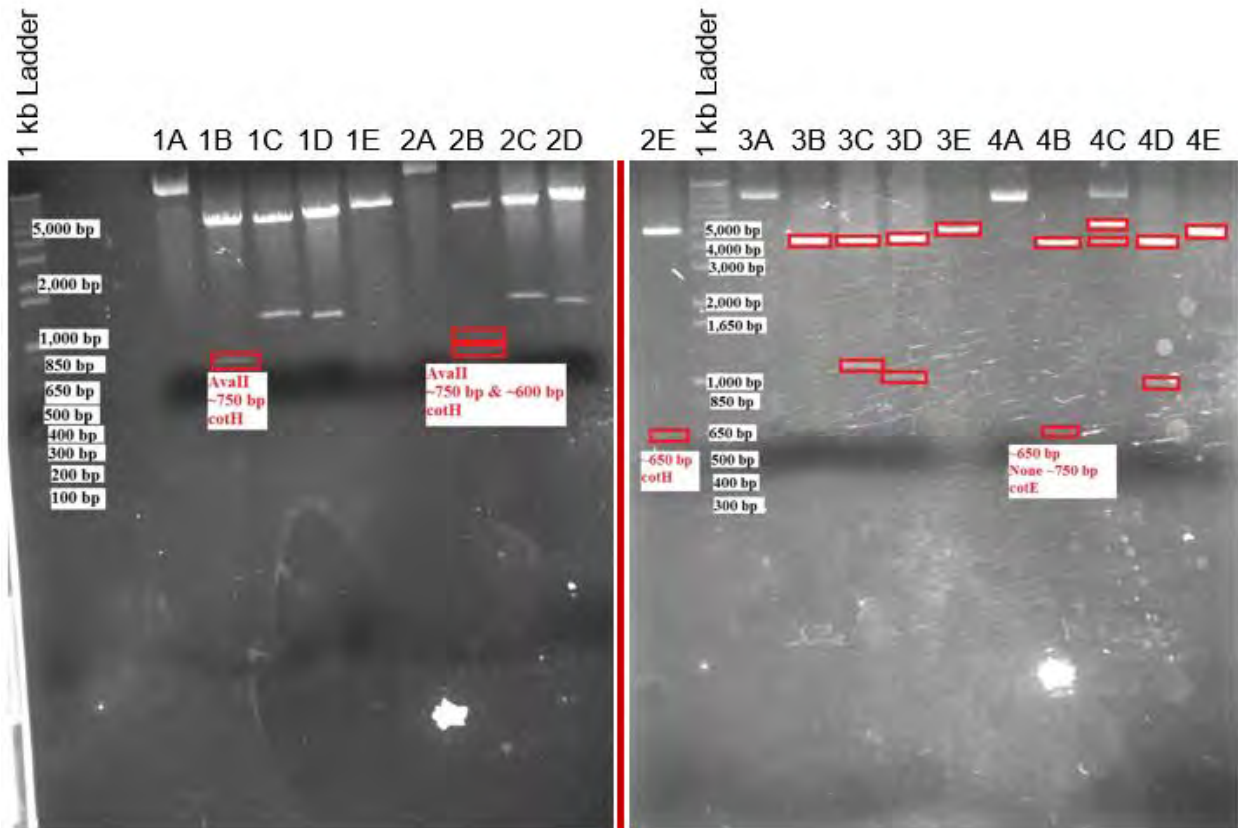


FIGURE 13. **Restriction Digests of Plasmid DNA Isolated from Minipreps.** Number corresponds to miniprep, letter corresponds to restriction digest. 1: Miniprep 1, 2: Miniprep 2, 3: Miniprep 3, 4: Miniprep 4. A: Negative control, B: *AvaII*, C: *BamHI*, D: *EcoRV*, E: *PstI* and *NotI*.

TABLE 2. **Expected Fragment Sizes for Miniprep Restriction Digests.**

	pNCCE1	pNCCH1	pNCC Backbone
Undigested	4,406	5,736	5,056
<i>AvaII</i>	70	70	70

	453	624	103
	624	783	624
	4,259	4,259	4259
BamHI	1,138	564	1,138
	4,268	1,138	3,918
		4,034	
EcoRV	1,025	215	1,025
	4,381	1,025	4,031
		4,496	
PstI and NotI	339	669	5,056
	5,067	5,067	

All fragment sizes in bp. Fragment sizes determined using NEBCutter V2.0 (Vincze et al. 2003).

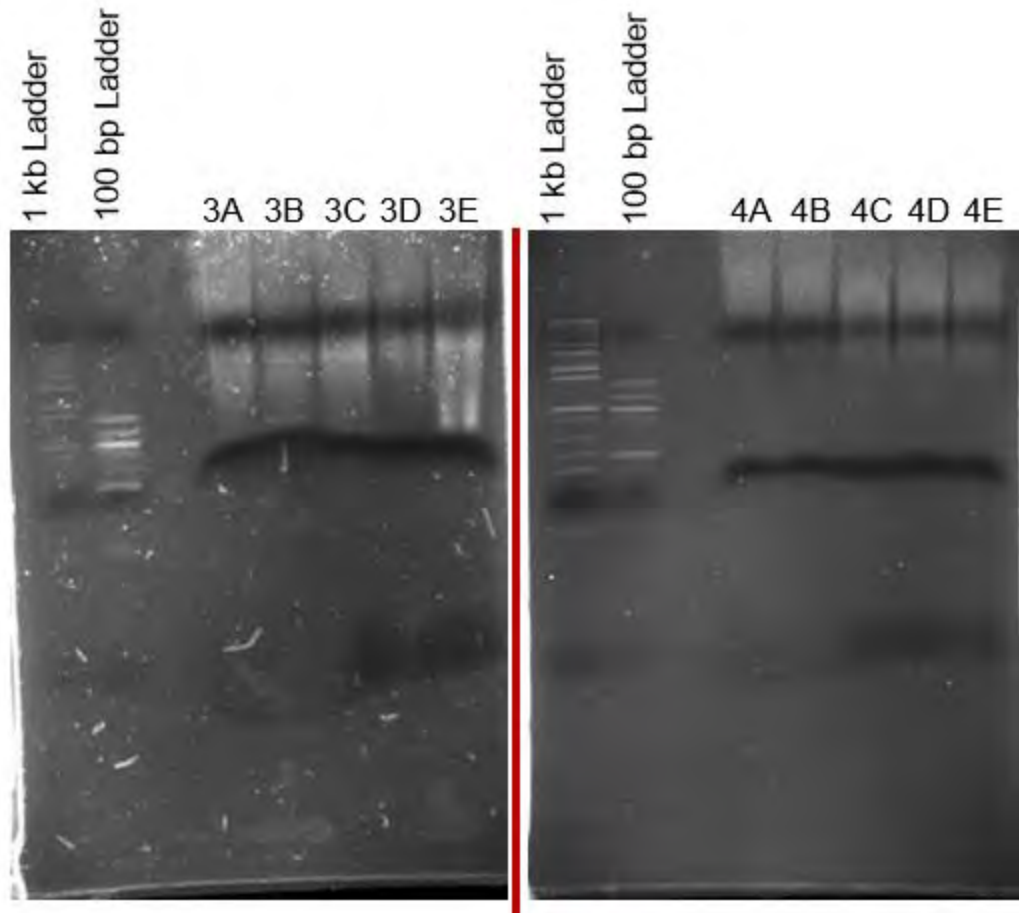


FIGURE 14. **Restriction Digests of Plasmid DNA Isolated from Midipreps.** Number corresponds to miniprep, letter corresponds to restriction digest. 3: Miniprep 3, 4: Miniprep 4. A: Negative control, B: *Ava*II, C: *Bam*HI, D: *Eco*RV, E: *Pst*I and *Not*I.

#### ACKNOWLEDGEMENTS

I thank Dr. Peterson for the *B. anthracis* str. Sterne genomic DNA and for pNCCH1 and for her constant assistance. I thank both Dr. Peterson, Dr. Visick, and Bronwen Heneghan for reviewing and commenting on this thesis. Thanks to North Central College, North Central College Summer Undergraduate Research, Dr. Driks, Dr. Peterson, and Dr. Visick for the opportunity to do this



research, and to the College Scholars Honors Program at North Central College for the opportunity to write this thesis.

## REFERENCES

- Active Motif, (2012) *RapidTrans<sup>TM</sup> 96-Tube Chemically Competent E. coli*, Ver. C2, Active Motif, Inc., Carlsbad, CA [online] [activemotif.com/documents/43.pdf](http://activemotif.com/documents/43.pdf)
- Alcaraz, L. D., Moreno-Hagelsieb, G., Eguiarte, L. E., Souza, V., Herrera-Estrella, L., and Olmedo, G. (2010) Understanding the evolutionary relationships and major traits of *Bacillus* through comparative genomics. *BMC Genomics*. 10.1186/1471-2164-11-332.
- Atrih, A., and Foster, S. J. (2002) Bacterial endospores the ultimate survivors. *Int. Dairy J.* **12**, 217-223.
- Beall, B., Driks, A., Losick, R., and Moran, Jr., C. P. (1993) Cloning and characterization of a gene required for assembly of the *Bacillus subtilis* spore coat. *J. Bacteriol.* **175**, 1705-1716.
- Boydston, J. A., Yue, L., Kearney, J. F., and Turnbough, Jr., C. L. (2006) The ExsY protein is required for complete formation of the exosporium of *Bacillus anthracis*. *J. Bacteriol.* **188**, 7440-7448.
- Bressuire-Isoard, C., Bornard, I., Henriques, A. O., Carlin, F., and Broussolle, V. (2016) Sporulation temperature reveals a requirement for CotE in the assembly of both the coat and exosporium layers of *Bacillus cereus* spores. *Appl. Environ. Microbiol.* **82**, 232-243.

CLUSTALW, Kyoto University Bioinformatics Center, Kyoto, Japan.

Donovan, W., Zheng, L., Sandman, K., and Losick, R. (1987) Genes encoding spore coat

polypeptides from *Bacillus subtilis*. J. Mol. Biol. **196**, 1-10.

Driks, A. (1999) *Bacillus subtilis* spore coat. Microbiol. Mol. Biol. Rev. **63**, 1-20.

Driks, A. (2002) Maximum shields: the assembly and function of the bacterial spore coat. Trends

Microbiol. **10**, 251-254.

Driks, A. (2004) The *Bacillus* spore coat. Phytopathology. **94**, 1249-1251.

Dworkin, J. (2014) Protein targeting during *Bacillus subtilis* sporulation. Microbiol. Spectr.

10.1128/microbiolspec.TBS-0006-2012.

Fazzini, M. M., Schuch, R., and Fischetti, V. A. (2010) A novel spore protein, ExsM, regulates

formation of the exosporium in *Bacillus cereus* and *Bacillus anthracis* and affects spore size and shape. J. Bacteriol. **192**, 4012-4021.

Galperin, M. Y. (2013) Genome diversity of spore-forming *Firmicutes*. Microbiol. Spectr.

10.1128/microbiolspectrum.TBS-0015-2012.

Ghosh, S., Setlow, B., Wahome, P. G., Cowan, A. E., Plomp, M., Malkin, A. J., and Setlow, P.

(2008) Characterization of spores of *Bacillus subtilis* that lack most coat layers. J.

Bacteriol. **190**, 6741-6748.

Giorno, R., Bozue, J., Cote, C., Wenzel, T., Moody, K.-S., Mallozzi, M., Ryan, M., Wang, R.,

- Zielke, R., Maddock, J. R., Friedlander, A., Welkos, S., and Driks, A. (2007) Morphogenesis of the *Bacillus anthracis* spore. *J. Bacteriol.* **180**, 691-705.
- GSL Biotech (2017) SnapGene, GSL Biotech LLC, Chicago.
- Henriques, A. O., and Moran, Jr., C. P. (2007) Structure, assembly, and function of spore surface layers. *Annu. Rev. Microbiol.* **61**, 555-588.
- Hyde, A. J., Parisot, J., McNichol, A., and Bonev, B. B. (2006) Nisin-induced changes in *Bacillus* morphology suggests a paradigm of antibiotic action. *Proc. Natl. Acad. Sci. U.S.A.* **103**, 19896-19901.
- Isticato, R., Pelosi, A., De Felice, M., and Ricca, E. (2010) CotE binds to CotC and CotU and mediates their interaction during spore coat formation in *Bacillus subtilis*. *J. Bacteriol.* **192**, 949-954.
- Kim, H., Hahn, M., Grabowski, P., McPherson, D. C., Otte, M. M., Wang, R., Ferguson, C. C., Eichenberger, P., and Driks, A. (2006) The *Bacillus subtilis* spore coat protein interaction network. *Mol. Microbiol.* **59**, 487-502.
- Liu, H., Bergman, N. H., Thomason, B., Shallom, S., Hazen, A., Crossno, J., Rasko, D. A., Ravel, J., Read, T. D., Peterson, S. N., Yates III, J., and Hanna, P. C. (2004) Formation and composition of the *Bacillus anthracis* endospore. *J. Bacteriol.* **186**, 164-178.
- Moir, A., and Smith, D. A. (1990) The genetics of bacterial spore germination. *Annu. Rev. Microbiol.* **44**, 531-553.

Naclerio, G., Baccigalupi, L., Zilhao, R., De Felice, M., and Ricca, E. (1996) *Bacillus subtilis* spore coat assembly requires *cotH* gene expression. J. Bacteriol. **178**, 4375-4390.

NCBI Resource Coordinators (2016) Database resources of the National Center for Biotechnology Information. Nucleic Acids Res. **44(Database issue)**, D7-D19. Doi: 10.1093/nar.gkv1290.

*NEB Cloner: RE Digest*, New England BioLabs, Ipswich, MA

New England BioLabs, Ligation Protocol with T4 DNA Ligase (M0202) [www.neb.com](http://www.neb.com) [online] [neb.com/protocols/1/01/01/dna-ligation-with-t4-dna-ligase-m0202](http://neb.com/protocols/1/01/01/dna-ligation-with-t4-dna-ligase-m0202)

Nicholson, W. L., Munakata, N., Horneck, G., Melosh, H. J., and Setlow, P. (2000) Resistance of *Bacillus* endospores to extreme terrestrial and extraterrestrial environments. Microbiol. Mol. Biol. Rev. **64**, 548-572.

Okyenwoke, R. U., Brill, J. A., Farahi, K., and Wiegel, J. (2004) Sporulation genes in members of the low G+C Gram-positive phylogenetic branch (*Firmicutes*). Arch. Microbiol. **182**, 182-192.

Paget, M. A. (2015) Bacterial sigma factors and anti-sigma factors: structure, function and distribution. Biomolecules. **5**, 1245-1265.

Peterson, Nancy. Personal communication.

QIAGEN, (2012) *QIAGEN® Plasmid Purification Handbook*, QIAGEN, Germantown, MD

[online] [qiagen.com/us/resources/resourcedetail?id=46205595-0440-459e-9d93-50eb02e5707e&lang=en](http://qiagen.com/us/resources/resourcedetail?id=46205595-0440-459e-9d93-50eb02e5707e&lang=en)

- Riesenman, P. J., and Nicholson, W. L. (2000) Role of the spore coat layers in *Bacillus subtilis* spore resistance to hydrogen peroxide, artificial UV-C, UV-B, and solar UV radiation. *Appl. Environ. Microbiol.* **66**, 620-626.
- Sandman, K., Losick, R., and Youngman, P. (1987) Genetic analysis of *Bacillus subtilis* *spo* mutations generated by Tn917-mediated insertional mutagenesis. *Genetics.* **117**, 603-617.
- Schleifer, K. H., and Kandler, O. (1972) Peptidoglycan types of bacterial cell walls and their taxonomic implications. *Bacteriol. Rev.* **36**, 407-477.
- Shatalin, K. Y., and Neyfakh, A. A. (2005) Efficient gene inactivation in *Bacillus anthracis*. *FEMS Microbiol. Lett.* **245**, 315-319.
- Smolelis, A. N., and Hartsell, S. E. (1949) The determination of lysozyme. *J. Bacteriol.* **58**, 731-736.
- Vasudevan, P., Weaver, A., Reichert, E. D., Linnstaedt, S. D., and Popham, D. L. (2007) Spore cortex formation in *Bacillus subtilis* is regulated by accumulation of peptidoglycan precursors under the control of sigma K. *Mol. Microbiol.* **65**, 1582-1594.
- Vincze, T., Posfai, J., and Roberts, R.J. (2003) NEBcutter: a program to cleave DNA with restriction enzymes. *Nucleic Acids Res.* **31**, 3688-3691.
- Wang, A., and Ash, G. J. (2015) Whole genome phylogeny of *Bacillus* by feature frequency

profiles (FFP). *Sci. Rep.* **13644**, doi:10.1038/srep13644.

Waterhouse, A.M., Procter, J.B., Martin, D.M.A, Clamp, M. and Barton, G. J. (2009)

Jalview Version 2 - a multiple sequence alignment editor and analysis workbench.

*Bioinformatics* **25(9)**, 1189-1191. Doi: 10.1093/bioinformatics/btp033

*Web Primer, Saccharomyces Genome Database*, Stanford, CA.

Zheng, L., Donovan, W. P., Fitz-James, P. C., and Losick, R. (1988) Gene encoding a

morphogenic protein required in the assembly of the outer coat of the *Bacillus subtilis* endospore. *Genes Dev.* **2**, 1047-1054.

Zilhao, R., Naclerio, G., Henriques, A. O., Baccigalupi, L. Moran, Jr., C. P., and Ricca, E. (1999)

Assembly requirements and role of CotH during spore coat formation in *Bacillus subtilis*. *J. Bacteriol.* **181**, 2631-2633.

Zymo Research, *Instruction Manual: Zymoclean™ Gel DNA Recovery Kit*, Ver. 1.2.0, Zymo

Research Corp., Irvine, CA [online] [zymoresearch.com/dna/dna-clean-up/gel-dna-recovery/zymoclean-gel-dna-recovery-kit](http://zymoresearch.com/dna/dna-clean-up/gel-dna-recovery/zymoclean-gel-dna-recovery-kit)

Zymo Research, *Instruction Manual: Zyppy™ Plasmid Miniprep Kit*, Ver. 1.2.6, Zymo

Research Corporation, Irvine, CA [online] [zymoresearch.com/dna/plasmid-dna-purification/bacterial-plasmid/zyppy-plasmid-miniprep-kit](http://zymoresearch.com/dna/plasmid-dna-purification/bacterial-plasmid/zyppy-plasmid-miniprep-kit)